nature materials

LETTERS

PUBLISHED ONLINE: 29 FEBRUARY 2016 | DOI: 10.1038/NMAT4574

Thermal resistance at a solid/superfluid helium interface

Aymeric Ramiere[1†], Sebastian Volz[2] and Jay Amrit[1*]

Kapitza[1] in 1941 discovered that heat flowing across a solid in contact with superfluid helium (<2 K) encounters a strong thermal resistance at the interface. Khalatnikov[2] demonstrated theoretically that this constitutes a general phenomenon related to all interfaces at all temperatures, given the dependence of heat transmission on the acoustic impedance (sound velocity × density) of each medium. For the solid/superfluid interface, the measured transmission of heat is almost one hundred times stronger than the Khalatnikov prediction. This discrepancy could be intuitively attributed to diffuse scattering of phonons[3] at the interface but, despite several attempts[4–7], a detailed quantitative comparison between theoretical and experimental findings to explain the occurrence of scattering and its contribution to heat transmission had been lacking. Here we show that when the thermal wavelength λ of phonons of the less dense medium (liquid ^{4}He) becomes comparable to the r.m.s. surface roughness σ, the heat flux crossing the interface is amplified; in particular when $\sigma \approx 0.33\lambda$, a spatial resonant mechanism occurs, as proposed by Adamenko and Fuks[8]. We used a silicon single crystal whose surface roughness was controlled and characterized. The thermal boundary resistance measurements were performed from 0.4 to 2 K at different superfluid pressures ranging from saturated vapour pressure (SVP) to above ^{4}He solidification, to eliminate all hypothetical artefact mechanisms. Our results demonstrate the physical conditions necessary for resonant phonon scattering to occur at all interfaces, and therefore constitute a benchmark in the design of nanoscale devices[9,10] for heat monitoring.

In the textbook example of wave propagation across a smooth interface between two media of density ρ_1 and ρ_2, the transmission coefficient[11] at the interface is given by $\tau = 2Z_1/(Z_1 + Z_2)$, where the acoustic impedance of each medium $Z_i = \rho_i c_i$, with c_i being the wave speed in medium $i = (1, 2)$. In the acoustic mismatch (AM) theory for thermal boundary resistance, Khalatnikov[2] uses this transmission coefficient to characterize heat conductance carried by the different phonon branches (one longitudinal and two transverse) across an interface. The AM theory agrees well in general with the experimental findings, apart from the case where interfaces are strongly acoustically mismatched—for example, the lead/diamond interface[12] and the solid/superfluid helium-4 interface at low temperatures[3]. The anomalous thermal boundary Kapitza resistance for these cases can differ by almost two orders of magnitude from the AM theory predictions, which has triggered extensive studies over decades.

Heat and sound in non-metal solids are mechanical vibrations. Treating heat as sound, Adamenko and Fuks[8] (AF) ascribed the scattering of quantized vibrations of heat (phonons) to the scattering of sound waves from rough surfaces. In both cases, the localized surface roughness (characterized by the root mean square roughness height σ and characteristic dimension or correlation length ℓ of the roughness) and the phonon thermal wavelength λ of the less dense material play decisive roles in determining the nature of the

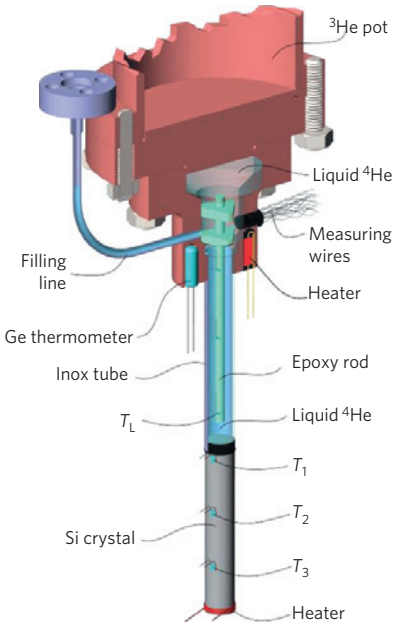

Figure 1 | Schematic representation of the experimental cell. The optically polished cross-sectional surface of a rod-shaped high-purity silicon single crystal is sealed superfluid-leak-tight into a thin-walled stainless steel tube. Three bare chipped RuO_2 (Model RX-102A-BR) thermometers (T_1, T_2, T_3) are equally spaced on the lateral surface of the crystal. They are sensitive to incident and reflected heat fluxes. A Manganin-wire heater (~64 Ω) supplies a heat flux which runs parallel along the *c*-axis of the crystal and crosses the [111] surface in contact with the superfluid. Liquid ^{4}He temperature (measured also by a RuO_2 thermometer, T_L) is regulated to within <1 mK with the aid of a calibrated Ge (GR-200A) thermometer and a 560 Ω carbon resistor (heater), which is fixed to the copper support of the cell. The superfluid pressure in the cell is monitored from the gas handling panel at room temperature and read on a Bourdon manometer.

[1]Laboratoire d'Informatique pour la Mécanique et les Sciences de l'Ingénieur, LIMSI-CNRS UPR 3251, Université Paris-Sud, Rue John von Neumann, 91405 Orsay, France. [2]Laboratoire Énergétique Moléculaire et Macroscopique Combustion, EM2C-CNRS UPR 288, École Centrale Paris, Grande voie des Vignes, 92295 Chatenay-Malabry, France. †Present address: LIMMS, UMI CNRS 2820-IIS, Center for International Research on MicroMechatronics, CIRMM, Institute of Industrial Science, University of Tokyo, 4-6-1 Komaba, Megruro-ku, Tokyo 153-8505, Japan. *e-mail: jay.amrit@limsi.fr

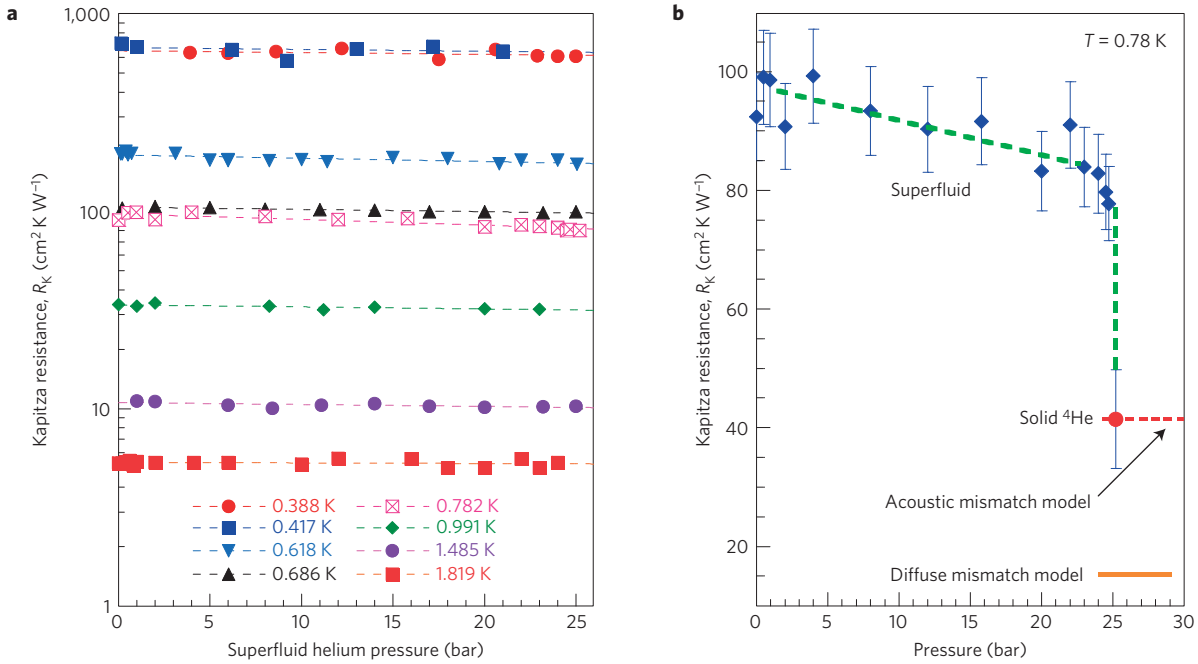

Figure 2 | Kapitza resistance R_K measurements. a, R_K shows no apparent dependence on the acoustic impedance of superfluid ^{4}He at different temperatures. The dashed lines are straight line fits to the data. **b**, Pressure dependence of R_K at the minimum temperature point (0.78 K) of the ^{4}He melting curve. The pressure is varied from SVP to above the solidification pressure (25 bar). R_K varies by nearly 12% (blue diamonds) before a first-order transition in R_K is seen (red circle) on the solidification of ^{4}He. The dashed green line is a guide to the eye to highlight these features. The error bars are mainly due to the relative uncertainties in the thermal conductivity of Si and in the temperature difference measurements. The AM model and the diffuse mismatch model predictions of R_K for the solid ^{4}He/Si interface are shown respectively by the dashed red line with the critical cone angle in solid ^{4}He, $\theta_C = 17°$ (Supplementary Information) and the orange line.

scattering. In the case of a solid/superfluid interface, Adamenko and Fuks show that when the roughness height follows a Gaussian distribution and when the condition $(\ell/\lambda) \approx 0.3$ is fulfilled, phonons become 'trapped' by roughnesses and a new resonant phonon mechanism becomes effective which carries a maximum amount of energy across the interface. The AF theory gained little attention and several works[13–15] up to now continue to speculate that the anomaly arises from a predominance of non-specular scattering of phonons by an unknown mechanism, still to be discovered.

Here we report a quantitative study which reveals the resonant phonon scattering mechanism proposed by Adamenko and Fuks; we demonstrate that when roughnesses of the order of a few nanometres become comparable in size to phonon wavelengths, resonant scattering is indeed dominant. The dominant wavelength of phonons in liquid helium[13] is given by $\lambda(P,T) = (hc_L(P)/3.83k_BT)$, where $c_L(P)$ is the pressure-dependent speed of sound[16] in helium and h is the Planck constant. By performing measurements at different pressures and temperatures we present a cross-check investigation of the roughness–wavelength relationship. This work provides a clear insight into the physical mechanism of heat transfer at the interface, clarifying the enigma of the Kapitza anomaly. The present work is also an examination of the phonon scattering from surfaces close to the ultimate high-frequency regime (~10 THz) found in room-temperature crystals. Indeed, the dominant wavelengths of phonons in liquid helium depend on $c_L(P)$, which is ~20 times smaller than the speed of sound in solid materials (~5,000 m s^{-1}). Therefore, λ in superfluid ^{4}He, which is of the order of ~1.5 nm at 2 K, is comparable to phonon wavelengths in solid thermal devices whose predominant phonon frequency lies in the ~10 THz range at room temperatures[17] and above. The surface roughness–wavelength interaction criterion established in this regime now becomes an essential tool for manipulating and controlling heat in nanoscale devices in general.

The most direct method to access the thermal boundary resistance is to measure the temperature difference across the interface in the presence of a heat flux. We use a similar method, but we instead regulate the temperature in liquid ^{4}He to maintain it to a constant value within <1 mK and measure the effect of phonon reflection at the interface on the thermometer T_1 as the heat flux $\dot{Q}$ across the interface is varied (see Fig. 1 and Supplementary Fig. 3 and Supplementary Information). The thermal boundary resistance is now given by $R_K(P,T) = \Delta T_1/(\Delta\dot{Q}/S_0)$, where the pressure in liquid ^{4}He is varied from saturated vapour pressure (SVP) to about 25 bar, S_0 is the ideally smooth cross-sectional area and ΔT_1 corresponds to the temperature change due to a modification in the heat flux $\Delta\dot{Q}$.

Our experiments were performed using a silicon single crystal with its (111) surface in contact with superfluid helium of ultrahigh purity (99.999%). The superfluid pressure above SVP is monitored by condensing ^{4}He from room temperature. Details of the experimental method for SVP pressure are given elsewhere[18]. Precautions were taken to ensure that the statistical properties of our sample surface fulfil the AF model requirements. As detailed further (see Methods), the AF model treats scattering from isotropic small-scale surface roughnesses having a roughness height–height correlation distribution which is Gaussian. The thermal conductance across the rough interface R_ζ^{-1}, normalized with respect to the conductance across an ideally smooth interface (Khalatnikov theory) R_{K0}^{-1}, is derived to be $R_\zeta^{-1}/R_{K0}^{-1} = 1 + (1/2)\gamma^2 f(\Theta)$, where $\gamma = (2\sigma/\ell)$ corresponds to the average inclination of roughness with $\sigma = \langle h^2 \rangle^{1/2}$, where $h = \zeta(r)$ at position $r = (x,y)$ and $f(\Theta)$ is a function representing the heat flux amplification depending on $\Theta = (\ell/\lambda)$. For an ideally smooth surface, σ and, therefore, γ equal zero, and hence the transmission is controlled by the acoustic impedances of each medium. When the second term is dominant, the transmission is controlled by both the roughness height σ and the correlation length ℓ of the solid surface, and also by the

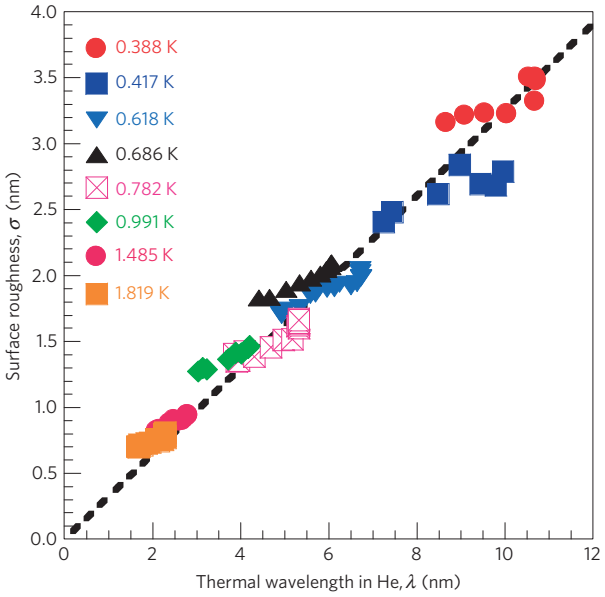

Figure 3 | Surface roughness σ dependence on the dominant thermal wavelength λ (in nm). The σ-values are determined from our R_K measurements using equation (1). The dashed line shows the condition $\sigma \approx 0.33\lambda$ for resonant scattering at the interface. Monitoring the superfluid ^{4}He pressure allows phonon wavelengths at different temperatures to be rendered identical (see Supplementary Information). This gives rise to the overlapping of some data points which corroborates the relationship between σ and λ for resonant scattering.

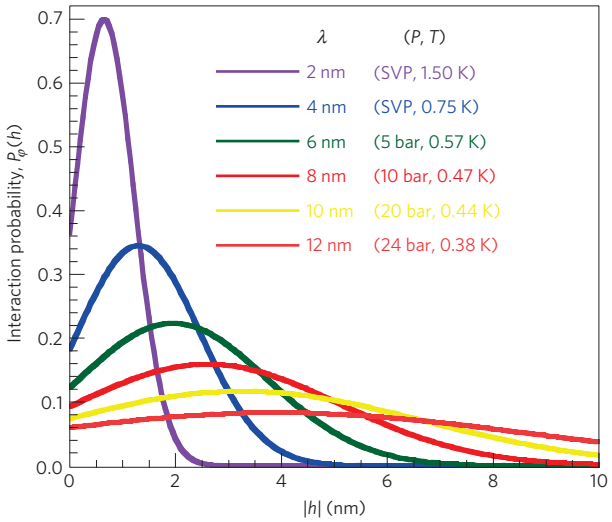

Figure 4 | Interaction probability $P_\varphi(h)$ for a phonon of wavelength λ to undergo resonant scattering from a roughness of height h. The calculations are performed for different λ values belonging to the temperature and pressure ranges of the experiment. A pair of (P, T) values for each wavelength λ is indicated. As $\lambda \propto c_L(P)/T$, different pairs of appropriately chosen (P, T) values yield identical λ values (see Supplementary Fig. 1 and Supplementary Information). As the temperature decreases and/or the pressure increases, $P_\varphi(h)$ decreases and covers an increasing range of h, indicating a gradual onset of specular scattering as the wavelengths increase. At very long wavelengths compared to h, the scattering becomes specular.

dominant thermal wavelength in liquid helium λ. It is important to note that both the mean inclination γ and $f(\Theta)$ independently play decisive roles for the resonant effect to be preponderant. Further, in the case of fine isotropic roughnesses studied here, $\ell < \lambda$ and $f(\Theta) = 115.5\Theta^2$ as $\Theta < 1$, and therefore R_ζ^{-1} now depends on σ and λ only, and can be written as (see equation (5), Methods):

$$\frac{R_\zeta^{-1}}{R_{K0}^{-1}} = 1 + 231\left(\frac{\sigma}{\lambda}\right)^2 \quad (1)$$

Figure 2a shows our measurements of the Kapitza resistance R_K, which were performed as a function of pressure (SVP to 25 bar) between 0.4 and 2 K. The results show that at a fixed temperature $T = 0.78$ K the change in the pressure of liquid He modifies R_K by nearly 12%, as seen in Fig. 2b. At $T > 1$ K, the effect of a pressure change is negligible (Fig. 2a). On the other hand, at a given pressure, R_K undergoes a change of approximately two orders of magnitude as the temperature is varied from 0.4 to 2 K. These results clearly show that the acoustic impedance of liquid He, which changes from $Z_L = 3{,}400\,\mathrm{g\,s^{-1}\,cm^{-2}}$ at SVP to $Z_L = 6{,}200\,\mathrm{g\,s^{-1}\,cm^{-2}}$ at 25 bar, has no detectable influence on the heat transmission at the interface.

In the AF theory the surface roughnesses σ which come into play in the resonant scattering mechanism are 'selected' by the thermal wavelengths in liquid ^{4}He. From our measurements, we determined the σ values using equation (1) with $\lambda(P, T)$. In Fig. 3, these σ values are plotted as a function of phonon wavelengths in liquid He. Each symbol corresponds to measurements done at a given temperature as the pressure is varied. The relationship between the surface roughness and the phonon wavelengths is strikingly evident. The straight line fitting our data clearly confirms the relationship $\sigma \approx 0.33\lambda$ as predicted by the AF theory for resonant scattering to occur. The overlapping of the data points at different temperatures and pressures confirms the role of He phonon wavelengths in the natural selection mechanism which favours resonant scattering. We also emphasize the fact that σ values which take part in the resonant scattering mechanism lie within the limited range 0.2–5 nm. The latter imposes a stringent condition on the robustness of the technique used to analyse surface roughness used to confirm the scattering mechanism.

To get a better understanding of the resonant scattering mechanism, the probability $P_\varphi(h)$ for a phonon to interact with a roughness height h is calculated following a normal distribution (see Methods). In Fig. 4 we illustrate $P_\varphi(h)$ for different λ values accessible in the pressure and temperature range of the experiment (see Supplementary Information). As seen from Fig. 4, for $\lambda = 2$ nm (high-frequency acoustic phonons in liquid He), $P_\varphi(\sigma(\lambda))$ attains ~70% and has a sharp narrow width peak centred on $h \approx 1$ nm. The predominance of resonant scattering here is understood by the fact that the scattering is responsive to roughness heights of ~1–2 nm only. Consequently, larger roughnesses do not induce resonant phonon scattering. At lower temperatures and/or higher pressures, λ increases (as acoustic frequencies decrease) and $P_\varphi(\sigma(\lambda))$ decreases. Phonons are now sensitive to a broader range of h values up to a limit of ~10 nm in our experiment. The sensitivity of the scattering mechanism to the surface roughness is clearly illustrated by the strong decrease in $P_\varphi(\sigma(\lambda))$ from ~70 to ~10% for a wavelength change from 2 to 12 nm, as seen in Fig. 4.

The surface roughness power spectral density (PSD) is the Fourier transform of the height–height correlation function at each scale length. By performing PSD analysis from atomic force microscopy (AFM) images made at various locations on our sample surface, we corroborate the scale lengths of roughnesses which are effective in the scattering mechanism as predicted by the AF theory. A typical two-dimensional PSD of our sample surface over an area of 100 nm × 100 nm performed using the software WSxM (ref. 19) is shown in Fig. 5. For clarity, log(PSD[q]) is plotted as a function of d(in nm), rather than log(q), where $q = d^{-1}$ is the wavenumber of the surface roughness. For $d > 10$ nm the surface roughness saturates

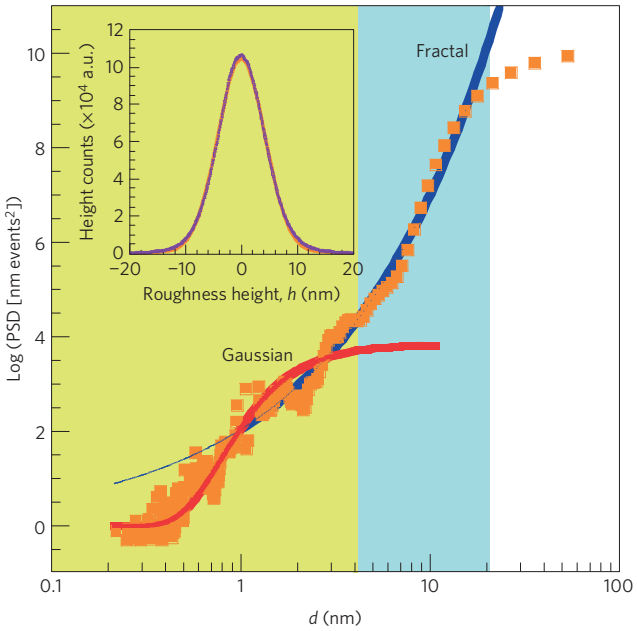

Figure 5 | Typical power spectral density (PSD) of our sample surface as a function of scale length *d*. In the green background, $d \leq 4$ nm and the data (orange) follow a Gaussian behaviour (red fit), justifying the applicability of the AF model. The blue background covers scale lengths $4 < d < 20$ nm, where a typical fractal behaviour (blue fit) is found for smooth Si surfaces. The inset shows AFM measurements (orange) and a fit (blue) to the roughness height distribution of our sample.

to a constant limit. This explains the onset of specular scattering as the temperatures are lowered below 0.5 K and as the wavelength becomes greater than 10 nm. The present analysis suggests that, even at lower temperatures (<0.3 K), a soft transition in the scattering nature is expected to lead to a fully specular regime.

For $d < 4$ nm the PSD data are fitted with a Fourier transform of the height–height correlation function, which now follows a Gaussian distribution and is given by $(\sigma^2_{\text{r.m.s.}}\ell^2/4\pi)\exp(-\ell^2/4d^2)$, with $\sigma_{\text{r.m.s.}} \approx 4.7$ nm and the correlation length $\ell \approx 1.5$ nm. We note that the fact that the Gaussian distribution is limited in the range $d < 4$ nm coincides remarkably with the interval of σ values (0.5–3.5 nm) predicted by the AF theory as shown in Fig. 3. In the intermediate domain where $4 < d < 10$ nm, the surface roughness has a characteristic fractal behaviour and our data are fitted with PSD $\propto d^{2-2H}$, where the Hurst exponent $H = 0.73$. The fractal behaviour is clearly not representative of the roughness behaviour when $d < 1$ nm and $d > 10$ nm.

To rule out the effect due to the presence of a hypothetical solid layer[7] of ^{4}He at the interface which would better adapt the acoustic impedance of liquid ^{4}He to that of silicon (see Supplementary Information), we performed the following experiment. We measured the interfacial resistance R_K at the minimum of the melting curve of ^{4}He (~0.778 K and ~25 bar; ref. 20) as the pressure in the superfluid was increased beyond the solidification pressure. The results are shown in Fig. 2b and exhibit a sharp drop in the Kapitza resistance from $R_{K,L} = (80 \pm 7)\,\text{cm}^2\,\text{K}\,\text{W}^{-1}$ at a pressure of 24.5 bar for the superfluid ^{4}He/Si interface to $R_{K,S} = (42 \pm 8)\,\text{cm}^2\,\text{K}\,\text{W}^{-1}$ after formation of solid helium at ~25.2 bar. The observed first-order transition is due to a physical change in the phonon transmission mechanism at the interface due to the presence now of transverse modes in both media. It is a clear signature that a layer of solid He, due to a van der Waals potential, if present before solidification, cannot be part of an impedance matching mechanism to explain discrepancies between our measurements of R_K (Fig. 2a) and the AM model predictions for solid–superfluid interfaces. For our value of $R_{K,S}$ to be in good agreement with the AM model, the critical cone angle in solid ^{4}He must be extended from $\theta_c \approx 3°$ (determined by the sound velocities of each medium) to $\theta_c \approx 17°$ (see Supplementary Information).

In conclusion, the interpretation of our experimental data using the AF model of resonant scattering of phonons from nanoscale surface roughness is fully corroborated by the surface analysis of our Si sample. This explanation is a significant step in understanding resonant phonon scattering at surfaces and fully accounts for the discrepancies among the multitude of experimental studies at low temperatures. To quantify the pressure effect on R_K at a given temperature is important, as it confirms the surface roughness–wavelength dependency in the resonant scattering mechanism. The observation of a transition in R_K with the solidification of ^{4}He is convincing proof of the absence of an effect due to a few atomic layers thickness of solid He, before solidification of liquid ^{4}He. Future work at high pressure has to be performed to understand our experimental value of R_K between solid ^{4}He and silicon, as quantum effects, dislocations and defects present in solid ^{4}He may certainly impact heat flow at the interface. Above all, the veracity of the AF theory in interpreting heat transmission at solid/superfluid ^{4}He interfaces is now demonstrated, unravelling almost 70 years of research on the origin of the anomalous Kapitza resistance.

Methods

Methods and any associated references are available in the online version of the paper.

Received 27 July 2015; accepted 19 January 2016; published online 29 February 2016

References

1. Kapitza, P. L. The study of heat transfer in helium II. *J. Phys.* **4,** 181–210 (1941).
2. Khalatnikov, I. M. *An Introduction to the Theory of Superfludity* (Addisson-Wesley, 1989).
3. Swartz, E. T. & Pohl, R. O. Thermal boundary resistance. *Rev. Mod. Phys.* **61,** 605–668 (1989).
4. Wyatt, A. F. G. & Crisp, G. N. Frequency of phonons emitted into liquid He by a solid. *J. Phys.* **39,** C6–C244 (1978).
5. Little, W. A. Unimportance of surface roughness upon the Kapitza resistance. *Phys. Rev. Lett.* **123,** 1909–1911 (1961).
6. Sheard, F., Bowley, R. M. & Toombs, G. A. Microscopic theory of the Kapitza resistance at a solid–liquid ^{4}He interface. *Phys. Rev. A* **8,** 3135–3145 (1973).
7. Challis, L., Dransfeld, K. & Wilks, J. Heat transfer between solids and liquid helium II. *Proc. R. Soc. Lond.* **260,** 31–46 (1961).
8. Adamenko, I. N. & Fuks, I. M. Roughness and thermal resistance of the boundary between a solid and liquid helium. *Sov. Phys. JETP* **32,** 1123–1129 (1971).
9. Wen, Y.-C. *et al*. Specular scattering probability of acoustic phonons in atomically flat interfaces. *Phys. Rev. Lett.* **103,** 264301 (2009).
10. Hochbaum, A. I. *et al*. Enhanced thermoelectric performance of rough silicon nanowires. *Nature* **451,** 163–167 (2008).
11. Pain, H. J. *The Physics of Vibrations and Waves* (John Wiley, 1983).
12. Stoner, R. J. & Maris, H. J. Kapitza conductance and heat flow between solids at temperatures from 50 to 300 K. *Phy. Rev. B* **48,** 16373–16387 (1993).
13. Nakayama, T. in *Prog. Low Temp. Phys.* Vol. XII, 115 (Elsevier, 1989).
14. Adamenko, I., Nemchenko, K. & Tanatarov, I. Transmission and reflection of phonons and rotons at the superfluid helium-solid interface. *Phys. Rev. B* **77,** 174510 (2008).
15. Adamenko, I. N. & Nemchenko, E. K. Heat Flow from solid to liquid He II due to inelastic processes of phonons interaction. *J. Low Temp. Phys.* **171,** 266–272 (2012).
16. Brooks, J. S. & Donnelly, R. J. The calculated thermodynamic properties of superfluid helium-4. *J. Phys. Chem. Ref. Data* **6,** 51–104 (1977).
17. Maldovan, M. Sound and heat revolutions in phononics. *Nature* **503,** 209–217 (2013).
18. Amrit, J. Impact of surface roughness temperature dependency on the thermal contact resistance between Si(111) and liquid ^{4}He. *Phys. Rev. B* **81,** 054303 (2010).

19. Horcas, I. *et al*. WSxM: a software for scanning probe microscopy and a tool for nanotechnology. *Rev. Sci. Instrum.* **78,** 1–8 (2007).
20. Grilly, E. R. Pressure-volume-temperature relations in liquid and solid ^{4}He. *J. Low Temp. Phys.* **11,** 33–52 (1973).

Acknowledgements
This work received partial financial aid from the LabEx LaSIPS of the Paris-Saclay University. We express our deep gratitude to the Institute of Nuclear Physics in Orsay for technical support. A.R. benefited from a grant from the Ministry of Education via ED 543 MIPEGE. We acknowledge discussions with I. N. Adamenko.

Author contributions
A.R. and J.A. ran the experiments. A.R., S.V. and J.A. analysed the data, performed the calculations and wrote the manuscript.

Additional information
Supplementary information is available in the online version of the paper. Reprints and permissions information is available online at www.nature.com/reprints. Correspondence and requests for materials should be addressed to J.A.

Competing financial interests
The authors declare no competing financial interests.

Methods

Resonant scattering model summary. The key features of the AF model are summarized here. A phonon, characterized by a monochromatic wave $\varphi_i = \varphi_o(z)e^{i(k.r-\omega t)} = \varphi_o(r,z)e^{-i\omega t}$, is incident from liquid helium (medium 1) on a rough solid surface. The roughness fluctuation height distribution is described by $\zeta(r)$, where $r=(x,y)$ is the position in the (x,y) plane. Part of the incident wave is reflected back into medium 1 and part of the wave is refracted into medium 2 (solid), and each contribution is defined respectively by $\varphi_r(r,z)e^{-i\omega t}$ and $\varphi_2(r,z)e^{-i\omega t}$. To calculate the transmission coefficient, the AF model follows the same procedure as in the Khalatnikov model for an ideal interface, but with the following new boundary conditions:

$$(\partial\varphi_1/\partial z - \partial\varphi_2/\partial z) - j\nabla_r(\varphi_1-\varphi_2)=0 \quad (2)$$

$$\rho_1\varphi_1 - \rho_2\varphi_2 = 0 \quad (3)$$

where $\varphi_1=\varphi_o+\varphi_r$ and $j=\nabla_r\zeta$ defines the roughness inclination at position r. Equation (2) imposes the continuity of the normal component of the velocity ϑ_z at $z=\zeta(r)=0$, which now is modified to take into account the surface roughness. Equation (3) is obtained from the usual continuity of the pressure gradient at $z=\zeta(r)=0$. It is important to note that a general treatment from arbitrarily rough surfaces is extremely complex and Adamenko and Fuks limit their calculations to isotropic small-scale surface irregularities for which $k\ell<1$ (or $(\ell/\lambda)<1$), where ℓ is the characteristic roughness length and the wavevector $k=(2\pi/\lambda)$, with λ being the thermal wavelength. Therefore, a perturbation theory approach is justified and the wave potentials are Taylor expanded up to quadratic powers of ζ, that is, $\varphi_m(r,\zeta)=\varphi_m(r,0)+(\partial\varphi_m/\partial z)\zeta+(\partial^2\varphi_m/\partial z^2)\zeta^2$, where $m=(1,2)$. Substitution in expressions (2) and (3) leads to integral equations for the amplitudes of φ_m in powers of ζ. Now the average transmission coefficient $\tau_\zeta(k,\theta)$ is given by the ratio of the power per unit area crossing the interface $\langle p(r,z)\vartheta_z(r,z)\rangle=(\rho_2\omega/2)\langle|\varphi_2|^2\rangle$ to the incident power per unit area $E_{inc}=\rho_1\omega/2$. We note that $p(r,z)$ is the local pressure. Thus, $\tau_\zeta(k,\theta)\propto(\rho_2/\rho_1)\langle|\varphi_2|^2\rangle$ and it contains dependencies on thermal frequencies (wavelengths) of phonons and surface roughness $\zeta(r)$. An explicit form for $\tau_\zeta(k,\theta)$ requires the surface properties to be statistically described. Under the assumption of isotropic small-scale roughness indicated above, the height–height roughness autocorrelation function is chosen to follow a Gaussian distribution—that is, $\langle\zeta(r)\zeta(r+d)\rangle=\sigma^2W(d)$, where $W(d)=e^{-d^2/\ell^2}$. The transmission coefficient of an incoming phonon of wavevector k, averaged over all incident angles θ, is calculated to be $F(k)=(2/3)[1+0.5\gamma^2\psi(k\ell)]$, where $\gamma=(2\sigma/\ell)$ and $\psi(k\ell)$ represents the increase in the transmission depending on k and ℓ. The heat flux entering the solid is given by the usual expression, now written as:

$$\dot{Q}_\zeta = \frac{2hc_L}{(2\pi)^3c_t^3}\left(\frac{\rho_1}{\rho_2}\right)\int_0^\infty n(\hbar c_L k/k_B T)F(k)k^3\,dk$$

where c_t is the transverse sound velocity in the solid and $n(\hbar c_L k/k_B T)$ is the Planck distribution for phonons in liquid He. Normalizing with respect to Khalatnikov's expression for the heat flux $\dot{Q}_0$ across an ideally smooth surface leads to $\dot{Q}_\zeta/\dot{Q}_0=1+(1/2)\gamma^2\omega(\Theta)$, where $\omega(\Theta)\propto\gamma^2\int_0^\infty n(k\ell/\Theta)\psi(k\ell)k^3\,dk$ defines the temperature and pressure dependency of phonon scattering by roughnesses and $\Theta=(\ell/\lambda)$ represents the dimensionless temperature. The resonant heat flux $\omega(\Theta)$ increases with Θ to reach a maximum when the phonon wavelength is three times the correlation length, that is, $(\ell/\lambda)\approx0.33$. Using the definition $R_K^{-1}=d\dot{Q}/dT$, the thermal boundary resistance across a rough interface normalized with respect to that of an ideally smooth interface takes the general form:

$$\frac{R_\zeta^{-1}}{R_{K0}^{-1}} = 1+\frac{1}{2}\gamma^2 f(\Theta) \quad (4)$$

where $f(\Theta)$ expresses temperature and pressure variations of $\omega(\Theta)$. When $(k\ell/2)<1$, that is $\Theta=(\ell/\lambda)<0.3$, AF calculations yield $\psi(k\ell)\approx0.75(k\ell)^2$ and $f(\Theta)\approx115.5\Theta^2$, where the numerical coefficient is due to constants, independent of temperature and pressure. Now, the thermal boundary resistance due to all phonon modes can be written in the form:

$$\frac{R_\zeta^{-1}}{R_{K0}^{-1}} = 1+57.75\gamma^2\left(\frac{\ell}{\lambda}\right)^2 \quad (5)$$

The first term corresponds to non-resonant modes. In the second term, the (ℓ/λ) ratio 'tunes' the degree of resonance scattering. As there is a distribution of wavelengths (and also a distribution of surface roughnesses), the resonance leads to a superposition of scattered waves which diffract into the solid, carrying energy into it.

Probability of phonon–roughness interactions $P_\varphi(h)$. The probability $P_\varphi(h)$ of phonons having a dominant wavelength λ to interact with a given roughness height h is calculated to follow a normalized Gaussian distribution centred at the mean expectation value $\sigma(\lambda)$ such that $P_\varphi(h)=1/\sqrt{2\pi}w\exp[-\{h-\sigma(\lambda)\}^2/2w^2]$, where w is the standard deviation or width of the Gaussian and $\sigma(\lambda)$ is given in Fig. 3. The w associated with a value of $\sigma(\lambda)$ is calculated using the roughness height distribution $\zeta(h)$ (see inset in Fig. 5) obtained by AFM. For a given value of $\sigma(\lambda)$, we truncate $\zeta(h)$ symmetrically to zero such that the root mean square roughness height $\langle h^2\rangle^{1/2}$ of the truncated histogram $\zeta'(h)$ reaches the value of $\sigma(\lambda)$. The total width of $\zeta'(h)$ now corresponds to $2w$. This ensures that ~95% of the phonons interact with roughness heights h confined within $\sigma(\lambda)\pm2w$.

Helium-4 crystal growth and measurement technique. The melting curve of helium-4 has a dip of approximately 8 mbar at a temperature of (0.775 ± 0.012) K and a pressure of (24.985 ± 0.005) atm (ref. 20). For temperatures above the minimum point, the pressure in the cell (read on a Bourdon manometer) is monitored directly by condensing helium through the gas handling system. The gas goes through a nitrogen trap before injection into the cell. To ensure that solid helium forms in the cell and on the Si surface, the superfluid ^{4}He in the cell is first pressurized to ~22 bar. Then a small heat flux (~30 μW) is applied across the interface and maintained constant throughout this experiment. The helium temperature T_L is now controlled to within ~1 mK to the minimum temperature as the pressure in the cell is increased at a rate not exceeding ~0.2 bar per minute with the aid of a needle valve. The crystallization of ^{4}He is clearly observed, as it causes a temperature shift on all thermometers. The estimated crystal growth rate does not exceed ~0.48 mm min^{-1}. This filling rate condition is respected so as to obtain the best possible helium crystal quality[21]. At the minimum point there is no latent heat release; consequently, the total heat flux crossing the interface remains unaltered as He solid is grown. The temperature difference across the interface before and after solidification changes respectively from $\Delta T=(T_L-T_1)$ to $\Delta T'=(T_{SHe}-T_1')$, where T_{SHe} is the temperature of solid ^{4}He measured by thermometer T_L. This change is directly proportional to the change in R_K from $R_{K,L}$ to $R_{K,S}$ with the solidification of ^{4}He. The Kapitza resistance at the solid ^{4}He/Si interface is now given by $R_{K,S}=R_{K,L}\times(\Delta T'/\Delta T)$. We emphasize that the contribution due to the solid ^{4}He layer between the thermometer T_L and the interface does not exceed ~1 cm^2 K W^{-1} and corresponds to an error of less than 2.5%.

References

21. Balibar, S., Alles, H. & Parshin, Y. A. The surface of helium crystals. *Rev. Mod. Phys.* **77,** 317–370 (2005).